

Article

Oxidation of Glycerol in the Presence of Hydrogen Peroxide and Iron in Model Solutions and Wine. Potential Effects on Wine Color

V. Felipe Laurie, and Andrew L. Waterhouse

J. Agric. Food Chem., **2006**, 54 (13), 4668-4673 • DOI: 10.1021/jf053036p • Publication Date (Web): 25 May 2006

Downloaded from <http://pubs.acs.org> on February 28, 2009

More About This Article

Additional resources and features associated with this article are available within the HTML version:

- Supporting Information
- Links to the 3 articles that cite this article, as of the time of this article download
- Access to high resolution figures
- Links to articles and content related to this article
- Copyright permission to reproduce figures and/or text from this article

[View the Full Text HTML](#)



ACS Publications
High quality. High impact.

Oxidation of Glycerol in the Presence of Hydrogen Peroxide and Iron in Model Solutions and Wine. Potential Effects on Wine Color

V. FELIPE LAURIE^{†,§} AND ANDREW L. WATERHOUSE^{*,†}

Department of Viticulture and Enology, University of California, Davis, California 95616, and Centro Tecnológico de la Vid y el Vino, Facultad de Recursos Naturales, Universidad de Talca, Talca, Chile

Wine oxidation appears to include the formation of hydroxyl radical ($\cdot\text{OH}$), an exceptionally reactive and thus nonselective compound that might be involved in the production of important aldehydes and ketones. This experiment examined the $\cdot\text{OH}$ oxidation of glycerol, a major wine constituent, and thus a likely target of such oxidation, in model wine, generated by hydrogen peroxide and iron catalysis. The oxidation products generated were analyzed as their hydrazones using LC-DAD/MS. Glyceraldehyde and dihydroxyacetone were the main compounds identified, both of which were also observed in naturally aged and $\cdot\text{OH}$ -oxidized wines. As anticipated, the presence of ethanol in the model wine did not preclude the formation of these compounds. Additionally, when a young red wine was treated with these oxidation derivatives, a noteworthy increase in color was observed, most likely due to the formation of novel anthocyanin-based structures.

KEYWORDS: Glycerol; oxidation; iron; hydrogen peroxide; hydroxyl radical; wine; glyceraldehyde; dihydroxyacetone; Fenton

INTRODUCTION

Many of the changes observed in the composition of wine during aging, leading to the development and transformation of various flavor and colored compounds, are attributed to oxidation reactions (1). When oxygen dissolves in wine, an activation step is required for it to become reactive and thus initiate oxidation. It is not clear whether this activation responds initially to metals ions, light, free radicals, or their combination, but once activated, new, more reactive derivatives of oxygen such as hydroperoxyl radical ($\text{HO}_2\cdot$) and hydrogen peroxide (H_2O_2) can be formed, hence allowing a ladder of free radical mediated oxidation reactions to occur (2).

More than 100 years ago, Fenton (3) reported a strong oxidant effect of H_2O_2 when iron salts were present. Forty years later, Haber and Weiss (4) suggested that this effect was due to the formation of the very reactive hydroxyl radical (**Figure 1**). Since then, many studies have linked this radical with oxidative processes, but only recently have wine researchers acknowledged that this could be key in understanding wine oxidation and aging (5, 6). Small amounts of metal ions, originating from the grapes, dust residues, and contamination with nonstainless steel winemaking equipment, are ubiquitous in wine (1, 7). Hydrogen peroxide, on the other hand, is mainly generated by the reduction of oxygen under the presence of hydrogen-donating species such as phenolics or ascorbic acid (8). The

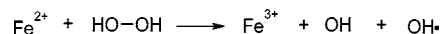


Figure 1. Fenton reaction.

essential function of metal catalysts in this process has been proposed and discussed elsewhere (2, 5).

The most widely accepted theory on the oxidation of wine phenolics (8) postulated that during their “autoxidation”, a strong oxidizing agent, namely, H_2O_2 , was generated, thus allowing the oxidation of ethanol to acetaldehyde. However, a recent report based on the observations of Fenton and Fenton and Jackson (3, 9) has stipulated that instead of H_2O_2 reacting directly as an oxidant, ferrous salts would catalyze a conversion to $\cdot\text{OH}$ (5). Due to the highly reactive nature of this radical, it is expected that all major oxidizable constituents of table and sweet wines, in proportion to their concentrations, would be oxidized as well (2). As with ethanol, many of the expected oxidation products of wine alcohols, sugars, and acids would be electrophilic aldehydes and ketones, substances that, aside from their possible aromatic impact, might react with phenolics and have potential effects on the color stability of wine as well as other effects. To date, a series of studies on the interaction between flavonoids and acetaldehyde (10–15) and between flavonoids and glyoxylic acid (an oxidation product of tartaric acid likely to arise from oxidation by hydroxyl radical) have been published (16, 17). It is also possible that part of the pyruvic acid that reacts with anthocyanins to create a stabilized pigment (18) could be formed by hydroxyl radical oxidation of malic acid.

A hurdle that must be overcome for these types of carbonyl compound mediated reactions to happen is the presence of high

* Corresponding author [fax (530) 752–0382; e-mail alwaterhouse@ucdavis.edu].

[†] University of California.

[§] Universidad de Talca.

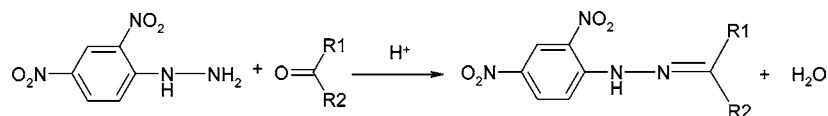


Figure 2. Reaction of 2,4-dinitrophenylhydrazine (DNPH) and aldehyde to form a stable hydrazone (R1, R2 = H, alkyl, aryl).

amounts of free sulfur dioxide (SO_2). When aldehydes and ketones react with bisulfite, the available amounts of both substrates in solution decrease. Additionally, carbonyl compounds react with alcohols to produce acetals and with nitrogen- and sulfur-containing compounds to produce various products (*I*, *7*). Consequently, the reactivity and volatility of aldehydes/ketones can be a problem for their quantitative analysis, although qualitatively, they can be effectively analyzed through their 2,4-dinitrophenylhydrazine (DNPH) derivatives (*20*, *21*) (**Figure 2**).

Given that glycerol is one of the most abundant chemical compounds in wine, with concentrations often higher than those typical for tartaric acid ($5\text{--}20\text{ g L}^{-1}$ for glycerol and $2\text{--}8\text{ g L}^{-1}$ for tartaric acid, which are approximately $54\text{--}217\text{ mM}$ for glycerol and $13\text{--}53\text{ mM}$ for tartaric acid) (*I*, *7*), and the lack of studies on its oxidation in wine or under wine-like condition, it seemed pertinent to focus on the oxidation of this substance. The aim of this study was to clarify whether glycerol is oxidized under wine conditions, identify its main oxidation products, and briefly evaluate the potential effects of these products on wine color.

MATERIALS AND METHODS

Reagents and Chemicals. Water purified through a Milli-Q system (Waters, Milford, MA) was used to prepare all solutions and dilutions. Glycerol (99.5%) was purchased from Sigma-Aldrich (Milwaukee, WI), whereas ethanol (100%) was purchased from Gold Shield Chemical Co. (Hayward, CA). A 30% hydrogen peroxide solution (EM Science/Merck, Whitehouse Station, NJ) and ferrous sulfate heptahydrate from Fisher (Fair Lawn, NJ) were used as the H_2O_2 and Fe^{2+} sources, respectively. pH corrections were attained with hydrochloric acid (1 N) from Fisher. Carbonyl compound derivatization was achieved by means of DNPH (30% water) from Alfa Aesar (Ward Hill, MA) and acetonitrile (HPLC grade) and perchloric acid (60%) from Fisher. Water, ammonium acetate (98.5% HPLC grade), and acetonitrile (HPLC grade) from Fisher were used for chromatography. Finally, a 99.5% acetaldehyde solution (Acros, Geel, Belgium), dl-glyceraldehyde (95%), and 1,3-dihydroxyacetone dimer (97%) purchased from Sigma-Aldrich, and mixtures of acetaldehyde–DNPH and formaldehyde–DNPH, obtained from AccuStandard (New Haven, CT), were used as standards for compound identification.

Model Solutions for Oxidation Experiments. Three different aqueous model solutions containing glycerol, ethanol, and their combination, as the primary solutes, were prepared as follows: (a) glycerol model solution, aqueous 7 g L^{-1} of glycerol acidified to pH 3.65 with 1 N hydrochloric acid; (b) ethanol model solution, aqueous 12% ethanol acidified to pH 3.65 with 1 N hydrochloric acid; (c) ethanol + glycerol model solution, aqueous 12% ethanol plus 7 g L^{-1} of glycerol adjusted to pH 3.66 with 1 N hydrochloric acid.

Treatments. Each of the above solutions (100 mL per replicate), in triplicate, was treated with the following: T1 (control), 25 μL of water; T2, 25 μL of water + 2.5 mg of ferrous sulfate, to give $\sim 5\text{ mg}$ of Fe^{2+} L^{-1} or 0.09 mM Fe^{2+} ; T3, 25 μL of 30% hydrogen peroxide, to give 0.075 mL of H_2O_2 L^{-1} or 2.54 mM H_2O_2 ; and T4, 25 μL of 30% hydrogen peroxide + 2.5 mg of ferrous sulfate. All samples were exposed to air by agitation for 2 min before and 2 min after the oxidizing agents were added.

All treatments were conducted in the dark and kept in amber bottles (50 mL) at room temperature ($24\text{ }^\circ\text{C}$) for the duration of the experiment. Adventitious metals, if any, were not removed prior the experiment, but their concentration was analyzed at the Interdisciplinary Center for Plasma Mass Spectrometry of the University of California at Davis

using an Agilent 7500ce inductively coupled plasma–mass spectrometer (ICP-MS). Samples were diluted by a factor of 1.25 for treatments T1 and T3 (without added iron) and by a factor of 10 for treatments T2 and T4 (with added iron) and spiked with the internal standard of germanium (Ge). Manganese, iron, copper, and zinc (and Ge) were analyzed using helium mode to reduce the effects of matrix interferences. Calibration was done using SPEX CertiPrep standards that range in concentration from 0.5 to 1000 ppb.

Glycerol, ethanol, and ethanol + glycerol model solutions were analyzed the same day ($t_{\text{day } 0}$), 1 day ($t_{\text{day } 1}$), 1 week ($t_{\text{day } 7}$), and 1 month ($t_{\text{day } 30}$) after the oxidizing treatments were applied. At $t_{\text{day } 0}$, the DNPH derivatization was done 1 h after the oxidizing agents had been dissolved into the model solutions.

DNPH Derivatization. DNPH solution was prepared by dissolving 200 mg of the DNPH reagent (30% water) in 100 mL of acetonitrile acidified with 4 mL of perchloric acid (60%) (*21*). The derivatizations of the model solutions and wine samples were performed by adding 1 mL of DNPH solution into 1 mL of sample. A reaction time of 3 h at room temperature was found to be enough for the derivatization of the main oxidation products of glycerol and ethanol. After 3 h, the samples were filtered through 0.45 μm polytetrafluoroethylene (PTFE), 13 mm, syringe tip filters (Arcodisc™) into 2 mL HPLC vials and sealed with PTFE crimp caps.

Liquid Chromatography–Electrospray Ionization/Mass Spectrometry Analyses. The chromatographic separation was achieved using a C18 LiChrospher column (4 mm \times 250 mm, 5 μm particle size) protected with a guard column of the same material. The mobile phase consisted of a binary gradient of (A) an aqueous 1 mM ammonium acetate and (B) 100% acetonitrile as follows: 0 min, 5% B; 5–15 min, 40% B; 20 min, 50% B; 25–45 min, 75% B; and 50–55 min, 5% B. The sample injection volume was 15 μL and the flow rate 0.2 mL min^{-1} . The chromatograph used was a Hewlett-Packard (HP) 1100 series, with a photodiode array UV–visible detector and an electrospray ionization mass spectrometry detector (HP 1100 MSD). UV–visible spectra were recorded from 200 to 600 nm. The MS was operated in negative-ion mode ($[\text{M} - \text{H}]^-$) with a capillary voltage of 3500 and fragmentor at 50 V. The drying gas flow was set at 12 L min^{-1} , the nebulizer pressure at 241.32 kPa, and the drying gas temperature at $350\text{ }^\circ\text{C}$.

Oxidized Wine Analysis. The occurrence of glycerol and ethanol oxidation products in wine was assessed by examining the LC-ESI/MS profile of four DNPH-derivatized white and red wine samples. Two naturally aged wines, a Chardonnay and a Cabernet Sauvignon from 1992, were compared with Sauvignon Blanc and Pinot Noir (2004) wines in which oxidation was induced by the combination of H_2O_2 and Fe^{2+} (same as T4). The ions with m/z of interest were extracted from their corresponding wine total ion chromatograms and were further compared. All wines were obtained from the wine library cellar at the University of California, Davis, CA.

Color Study. To briefly evaluate the potential effects of these products on wine color, a young red wine cv. Cabernet Sauvignon (2004) from Napa Valley, California [pH 3.88, and 14 and 29 mg L^{-1} free and total SO_2 , respectively, determined according to the method of aeration oxidation (*7*)], was treated with an excess of 0.5 g L^{-1} of dl-glyceraldehyde (5.55 mM) or 1 g L^{-1} 1,3-dihydroxyacetone dimer (5.55 mM) and compared to a control with no aldehyde addition (all samples were prepared in triplicate). Following the aldehyde additions, the replicated samples were kept at $37\text{ }^\circ\text{C}$ and analyzed after 1.5 h. Color changes were measured as the variation in absorbance at 420 and 520 nm, using an HP 8452A diode array spectrophotometer.

RESULTS AND DISCUSSION

Model Solution Oxidation Experiments. All chromatographic samples analyzed showed one main peak (labeled *I* with

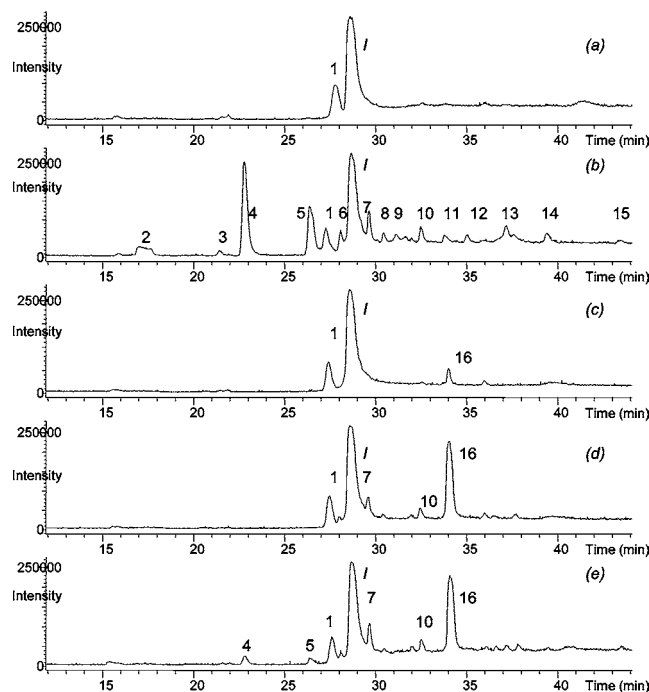


Figure 3. LC-ESI/MS chromatograms of DNPH derivatized (a) control glycerol solution, (b) $\text{H}_2\text{O}_2 + \text{Fe}^{2+}$ oxidized glycerol solution, (c) control ethanol solution, (d) $\text{H}_2\text{O}_2 + \text{Fe}^{2+}$ oxidized ethanol solution, and (e) $\text{H}_2\text{O}_2 + \text{Fe}^{2+}$ oxidized ethanol + glycerol solution. I = excess DNPH.

Table 1. Spectral Information on Oxidation Derivatives from Glycerol, Ethanol, and Ethanol plus Glycerol Oxidized ($\text{H}_2\text{O}_2 + \text{Fe}^{2+}$) Model Solution (at $t_{\text{day}0}$)

peak	RT (min)	$t_{\text{day}0}$	
		UV-vis $_{\text{max}}$ (nm)	$[\text{M} - \text{H}]^-$ (m/z)
1	27.27	366	238.2
I	28.66	354	197.2
2	17.61	363	183.2
3	21.45	338	225.2
4	22.78	363	269.2
5	26.38	368	269.2
6	28.08	362	239.2
7	29.63	345	182.2
8	30.45	361	239.2
9	31.12	nd	267.2
10	32.48	353	209.2
11	33.88	nd	363.3
12	35.05	351	389.5
13	37.18	442	447.3
14	39.40	440	417.3
15	43.50	440	431.3
16	34.07	362	223.2

a m/z of 197.2 for its main ion detected in $[\text{M} - \text{H}]^-$, corresponding to the excess hydrazine used to derivatize the carbonyl compounds, and a second unidentified peak, labeled 1, with m/z 238.3.

(a) *Glycerol Model Solution.* At $t_{\text{day}0}$, no major detectable peaks, other than I and 1, were observed for the control treatment (T1) (Figure 3a), the Fe^{2+} -added treatment (T2), and the H_2O_2 -added treatment (T3), whereas several peaks, 2–15, were evident when H_2O_2 and Fe^{2+} were added together (T4) (Figure 3b). Table 1 summarizes the spectral information of the peaks detected. Most peaks showed maximum absorptions between 345 and 370 nm, typical for single carbonyl group compounds, except for 13 (442 nm), 14 (440 nm), and 15 (440 nm), for which maximum visible absorbances might indicate more complex carbonyl-type compounds.

(b) *Ethanol Model Solution.* Other than I and 1, treatments T1 (control), T2 (Fe^{2+}), and T3 (H_2O_2) showed a small peak tagged 16, with m/z ratio 223.2, which remained as a contaminant from the ethanol utilized (Figure 3c). To corroborate the occurrence of this contaminant, a water sample and three ethanol solutions at increasing concentrations (10, 20, and 60%) were analyzed, showing a clear increase in this signal's response (data not shown). Treatment T4 ($\text{H}_2\text{O}_2 + \text{Fe}^{2+}$), on the other hand, showed significantly larger amounts of the prior compound (peak 16), along with a number of peaks, of which 10 and 7 were the most prominent (m/z 209.2 and 182.2, respectively) (Figure 3d; Table 1). Studies on ethanol oxidation have shown that $\cdot\text{OH}$ will abstract hydrogen atoms mainly at carbon 1, but the reaction at carbon 2 has also been suggested, allowing for several oxidation products to be generated (22).

(c) *Ethanol + Glycerol Model Solution.* As before, no changes in the chromatograms at $t_{\text{day}0}$ were observed for T1 (control), T2 (Fe^{2+}), and T3 (H_2O_2), whereas a combination of the same oxidation products previously observed for T4 ($\text{H}_2\text{O}_2 + \text{Fe}^{2+}$) was also detected here; hence, the presence of ethanol in higher molar concentration than glycerol suppressed but did not prevent the formation of the major oxidation products previously listed for the ethanol model solution. This result supports the theory that $\cdot\text{OH}$ might react with wine substances in proportion to their concentration and not necessarily on the basis of their hydrogen-donating ability. Due to its overwhelming concentration, ethanol is then expected to exert an important protective effect against the oxidation of other wine substrates, but glycerol and the hydroxyacids (tartaric, malic, and lactic acid), depending on their concentrations, should be important substrates as well. In this case, even though the molar concentration of ethanol was 27 times higher than those of glycerol (2.07 M and 76.01 mM respectively), its oxidation products were observed as well. Preliminary studies (data not shown) using tartaric acid as the buffer still yielded glyceraldehyde and dihydroxyacetone, but the multiple tartaric acid products complicated the chromatograms.

The major peaks observed for T4, other than I and 1, were those with m/z of 223.2, 209.2, 182.2, and 269.2 (Figure 3e; Table 1).

On the basis of the chemistry of the DNPH derivatization reaction (Figure 2) and assuming that most of these peaks are hydrazones (no or limited fragmentation information was obtained from the MS analyses), the m/z values attained can be used to calculate the molecular weights (MW) of the derivatized aldehydes or ketones as follows:

$$\text{hydrazone MW} + 1 [\text{M} - \text{H}]^- - \text{DNPH MW} + \text{H}_2\text{O MW} = \text{carbonyl compound MW}$$

Using the m/z of peak 4 (Figure 3b), as an example, 269.2 + 1 – 198.14 + 18.02, a molecular weight of 90.08 is obtained. The oxidation of glycerol is anticipated, and the likely products are glyceraldehyde and dihydroxyacetone (9), both of which have molecular weights of 90.08. The further oxidation and degradation of these compounds could generate a series of acids and other aldehydes including formaldehyde (molecular weight of 30.03) (Figure 4). When ethanol is part of the model solution, at least acetaldehyde (molecular weight of 44.06) and formaldehyde are expected as well.

To verify the aforementioned, standards of DL-glyceraldehyde, 1,3-dihydroxyacetone dimer, and acetaldehyde prepared in acidic water (pH 3.65) were derivatized under the same conditions formerly described and analyzed with LC-ESI/MSD. The

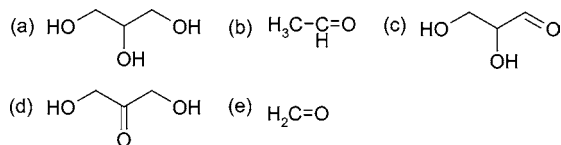


Figure 4. Chemical structures of (a) glycerol, (b) acetaldehyde, (c) glyceraldehyde, (d) dihydroxyacetone, and (e) formaldehyde.

Table 2. Metal Concentration in Samples of Ethanol plus Glycerol Model Solution^a

element	treatment									
	T1	SD	T2	SD	T3	SD	T4	SD	DL	
	($\mu\text{g L}^{-1}$)	(%)	($\mu\text{g L}^{-1}$)	(%)	($\mu\text{g L}^{-1}$)	(%)	($\mu\text{g L}^{-1}$)	(%)	($\mu\text{g L}^{-1}$)	($\mu\text{g L}^{-1}$)
Mn	0.11	2.7	9.2	0.8	0.11	5.0	15	1.0	0.004	
Fe	11	3.1	6.5×10^3	0.5	4.5	8.2	4.9×10^3	0.8	0.99	
Cu	0.36	1.7	0.6	5.6	0.35	2.6	0.31	1.2	0.004	
Zn	14.2	0.9	17	1.5	11	1.8	20	1.5	0.019	

^a T1, control; T2, Fe^{2+} addition; T3, H_2O_2 addition; T4, $\text{Fe}^{2+} + \text{H}_2\text{O}_2$ addition; DL, detection limit.

analysis was also applied to samples of commercially derivatized acetaldehyde and formaldehyde hydrazones. The retention times, mass spectra, and UV–vis spectra of these derivatives matched the retention times and ions formed for their corresponding peaks in all chromatograms (glyceraldehyde and dihydroxyacetone, peaks 4 and 5; acetaldehyde, peak 16; and formaldehyde, peak 10). Given that we were primarily interested in the detection and analysis of electrophilic reaction products and therefore used an analytical method limited to carbonyl compounds, we were unable to investigate whether other expected secondary products, mainly of acidic nature (oxalic acid, meso-oxalic acid, glyceric acid, glycolic acid, hydroxypyruvic acid, and tartronic acid) that have been observed in other model systems (23–26) are also produced under wine conditions.

As the reaction time between the oxidizing agents in T4 ($\text{H}_2\text{O}_2 + \text{Fe}^{2+}$) and the solutes used in all cases progressed ($t_{\text{day}1}$), there were noticeable rises in the apparent peak areas of the major analytes. These eventually reached a maximum and subsequently decreased between $t_{\text{day}7}$ and $t_{\text{day}30}$ (data not shown). This is believed to happen due to subsequent oxidation or rearrangement of the primary aldehyde/ketone products into other carbonyl or acids forms (25, 26). The significance of the timing and methodology used for the determination of oxidation derivatives should be emphasized, as the resulting compounds detected might vary depending on when and how the analyses were done. As for T3 (H_2O_2), the appearance of some oxidation products was noticed between $t_{\text{day}7}$ and $t_{\text{day}30}$, although with smaller apparent peak areas than in T4 ($\text{H}_2\text{O}_2 + \text{Fe}^{2+}$). In a study of the iron-catalyzed oxidation of (+)-catechin, Oszmianski et al. (27) observed evidence of oxidation in an “iron-free” treatment, with products different from those generated when iron was available. The authors interpreted these results as “iron-independent reactions” competing with those happening when iron was offered, although the possibility of metal contamination was not ruled out. In this regard, it has been stated that metal catalysts are the most likely source of activation energy for the strong oxygen-derived oxidation species to arise (2, 5). The analysis of metals performed for all model solution showed small but consistent amounts of iron, zinc, copper, and manganese (Table 2).

In brief, as originally reported by Fenton and Jackson in 1899 (9), the combination of H_2O_2 and Fe^{2+} (T4) showed a far stronger oxidizing power than H_2O_2 (T3) alone, whereas no oxidant effect was observed for the Fe^{2+} alone treatment (T2)

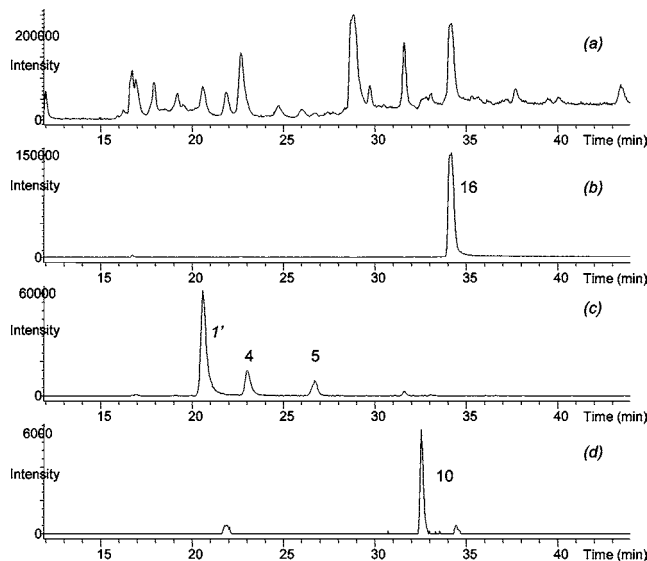


Figure 5. LC-MS chromatograms of (a) DNP-derivatized Chardonnay wine (vintage 1992) and extracted ions at (b) m/z 223.2, (c) m/z 269.2, and (d) m/z 209.2. Peak 16 corresponds to acetaldehyde, peaks 4 and 5 correspond to glyceraldehyde and dihydroxyacetone, respectively, peak 9 corresponds to formaldehyde, and 1' is an unknown peak.

or the control (T1). Additionally, the rapid increase in the number of peaks observed for all model solutions was attributed to the reactions of $\cdot\text{OH}$ and the hydrogen donor solutes in these solutions (glycerol, ethanol, and their oxidation derivatives). This seems to be a very important avenue of oxidation in wine that until now has not been systematically studied and requires more attention. It is yet to be clarified whether any of the secondary products reported in the literature (23–26) (oxalic acid, meso-oxalic acid, glyceric acid, glycolic acid, hydroxypyruvic acid, and tartronic acid) are also formed in acidic model solutions and wine.

Oxidized Wine Analysis. The m/z $[\text{M} - \text{H}]^-$ values corresponding to the main ions of glyceraldehyde, dihydroxyacetone, acetaldehyde, and formaldehyde DNP derivatives were extracted from the total ion chromatograms of all four wines analyzed (naturally aged and $\cdot\text{OH}$ -induced oxidized wines). In all cases, considerable amounts of m/z 223.2 (acetaldehyde) were observed, with smaller but detectable amounts of m/z 269.2 (glyceraldehyde and dihydroxyacetone) and 209.2 (formaldehyde) (see Figure 5 as an example). Coincidentally, a peak with the same m/z ratio as glyceraldehyde and dihydroxyacetone (m/z 269.2), appearing at 20.6 min, was observed, but its identity was not pursued.

In addition, to further demonstrate that glycerol can undergo oxidation in the presence of ethanol and tartaric acid, the peaks corresponding to glyceraldehyde and dihydroxyacetone (m/z 269.2) were extracted from the traces of a young wine and its $\cdot\text{OH}$ -oxidized counterpart (Figure 6). As observed, the areas of peaks 4 and 5 increased substantially in the oxidized wine.

Glyceraldehyde and dihydroxyacetone have been indicated as the first fermentation breakdown products of hexoses (1), but their abundances in wine have yet to be determined.

Color Study. In this simple experiment, both glyceraldehyde and dihydroxyacetone additions rapidly increased the absorbance values at 420 and 520 nm. Differences of 3.7% more absorbance at 420 nm and 7.4% more at 520 nm were observed 1.5 h after DL-glyceraldehyde was added. In contrast, 1,3-dihydroxyacetone additions resulted in absorbance increments of 3.1 and 3.7% at 420 and 520 nm, respectively (Figure 7). The reader should

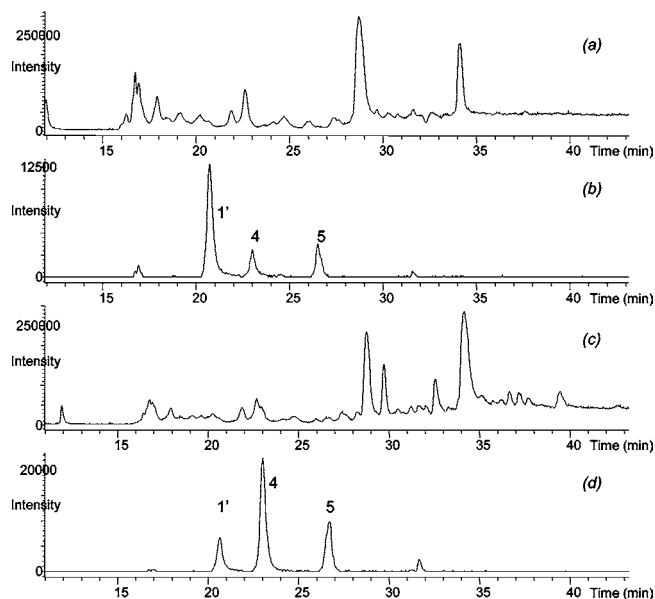


Figure 6. LC-MS chromatograms of (a) DNPH-derivatized Sauvignon Blanc wine (vintage 2004), (b) extracted ion m/z 269.2 from (a); (c) $\text{H}_2\text{O}_2 + \text{Fe}^{2+}$ oxidized (a); and (d) extracted ions m/z 269.2 from (c). Note higher scale for (d) relative to (b). Peak 1' is an unknown, peak 4 is glyceraldehyde, and peak 5 is dihydroxyacetone.

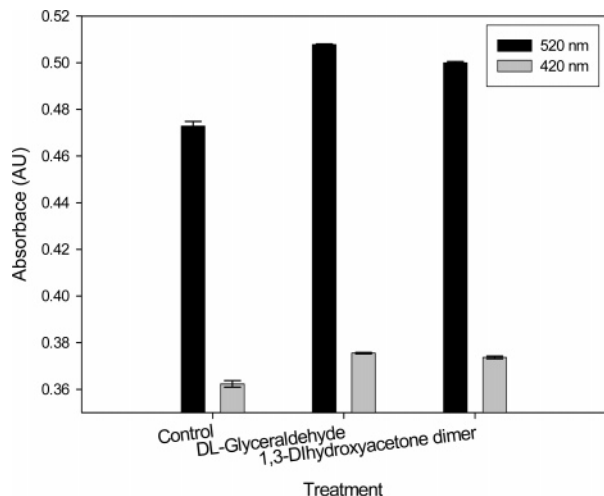


Figure 7. Absorbance values at 420 and 520 nm, after addition of DL-glyceraldehyde or 1,3-dihydroxyacetone dimer to a young red wine (Cabernet Sauvignon 2004). Error bars represent the standard deviation of three replicate samples each.

note that although the molar concentrations of the aldehydes used were the same, dihydroxyacetone was added as a dimer, and it is likely that not all of it was hydrolyzed to the reactive monomer form.

As previously shown elsewhere for acetaldehyde and glyoxylic acid, this type of wine color augmentation could be explained by the formation of condensed structures between flavonoids bridged by aldehydes or acids with carbonyl functional groups, these structures being more stable than monomeric anthocyanins (10, 16, 17). Significant observations in this regard have been those that established that condensation of catechin and malvidin-3-glucoside via acetaldehyde is faster at low pH and that temperature is a determinant factor in the development and accumulation of new pigments (28, 29). The possibility that this increase in color, or part of it, might have resulted from a disruption in the reversible equilibrium between anthocyanins

and sulfur dioxide (30), caused by the addition of the carbonyl compounds, should not be ruled out.

To conclude, these experiments suggest, for the first time, that other weak hydrogen donor species that exist at relatively high concentrations, such as acids, sugars, and polyols, could lead to additional oxidation products and play a significant role in wine aging. Because the oxidation of these substances leads to reactive electrophiles, their importance in aging could lie in their secondary products, after reaction with nucleophiles such as thiols or phenolics. Another important conclusion is that a predictive understanding of wine oxidation must take iron into account, but due to iron's multiple oxidation states and facile complexation with several wine substances, both of which would affect reactivity with hydrogen peroxide, a detailed analysis is essential.

ABBREVIATIONS USED

HPLC-DAD/MSD, high-performance liquid chromatography–diode array and mass spectrometry detection; LC-ESI/MSD, liquid chromatography–electrospray ionization mass spectrometry; UV–vis, ultraviolet–visible.

LITERATURE CITED

- (1) Ribéreau-Gayon, P.; Glories, Y.; Maujean, A.; Dubourdieu, D. *Handbook of Enology. The Chemistry of Wine Stabilization and Treatments*; Wiley: New York, 2000; Vol. 2. 404 pp.
- (2) Waterhouse, A. L.; Laurie, V. F. Oxidation of wine phenolics: a critical evaluation and hypotheses. *Am. J. Enol. Vitic.* **2006**, in press.
- (3) Fenton, H. J. H. Oxidation of tartaric acid in the presence of iron. *J. Chem. Soc.* **1894**, 75, 1–11.
- (4) Haber, F.; Weiss, J. J. The catalytic decomposition of hydrogen peroxide by iron salts. *Proc. R. Soc. London* **1934**, 147, 332–351.
- (5) Danilewicz, J. C. Review of reaction mechanisms of oxygen and proposed intermediate reduction products in wine: central role of iron and copper. *Am. J. Enol. Vitic.* **2003**, 54 (2), 73–85.
- (6) Boulton, R. B. A radical review of oxidation reactions in wine. *In IX Congreso Latinoamericano de Viticultura y Enología*; Pszczółkowski, Ph., Ed.; Pontificia Universidad Católica de Chile: Santiago, Chile, 2003; pp 107–133.
- (7) Ough, C. S.; Amerine, M. A. *Methods for Analysis of Must and Wines*, 2nd ed.; Wiley: New York, 1988; 377 pp.
- (8) Wildenrad, H. L.; Singleton, V. L. The production of aldehydes as a result of oxidation of polyphenolic compounds and its relation to wine aging. *Am. J. Enol. Vitic.* **1974**, 25 (2), 119–126.
- (9) Fenton, H. J. H.; Jackson, H. The oxidation of polyhydric alcohols in presence of iron. *J. Chem. Soc., Trans.* **1899**, 75, 1–11.
- (10) Timberlake, C. F.; Bridle, P. Interactions between anthocyanins, phenolic compounds, and acetaldehyde and their significance in red wines. *Am. J. Enol. Vitic.* **1976**, 27 (3), 97–105.
- (11) Fulcrand, H.; Doco, T.; Essafi, N. E.; Cheynier, V.; Moutounet, M. Study of the acetaldehyde induced polymerization of flavan-3-ols by liquid chromatography ion spray mass spectrometry. *J. Chromatogr. A* **1996**, 752 (1–2), 85–91.
- (12) Bakker, J.; Timberlake, C. F. Isolation, identification, and characterization of new color-stable anthocyanins occurring in some red wines. *J. Agric. Food Chem.* **1997**, 45, 35–43.
- (13) Saucier, C.; Guerra, C.; Pianet, I.; Laguerre, M.; Glories, Y. (+)-Catechin-acetaldehyde condensation products in relation to wine-aging. *Phytochemistry* **1997**, 46 (2), 229–234.
- (14) Es-Safi, N. E.; Fulcrand, H.; Cheynier, V.; Moutounet, M. Competition between (+)-catechin and (–)-epicatechin in acetaldehyde-induced polymerization of flavanols. *J. Agric. Food Chem.* **1999**, 47, 2088–2095.

- (15) Es-Safi, N. E.; Fulcrand, H.; Cheynier, V.; Moutounet, M. Studies on the acetaldehyde-induced condensation of (–)-epicatechin and malvidin 3-O-glucoside in a model solution system. *J. Agric. Food Chem.* **1999**, *47*, 2096–2102.
- (16) Es-Safi, N. E.; Le Guerneve, C.; Cheynier, V.; Moutounet, M. New phenolic compounds formed by evolution of (+)-catechin and glyoxylic acid in hydroalcoholic solution and their implication in color changes of grape-derived foods. *J. Agric. Food Chem.* **2000**, *48*, 4233–4240.
- (17) Fulcrand, H.; Cheynier, V.; Oszmianski, J.; Moutounet, M. An oxidized tartaric acid residue as a new bridge potentially competing with acetaldehyde in flavan-3-ol condensation. *Phytochemistry* **1997**, *46* (2), 223–227.
- (18) Fulcrand, H.; Benabdeljalil, C.; Rigaud, J.; Cheynier, V.; Moutounet, M. A new class of wine pigments generated by reaction between pyruvic acid and grape anthocyanins. *Phytochemistry* **1998**, *47* (7), 1401–1407.
- (19) Vogel, M.; Buldt, A.; Karst, U. Hydrazine reagents as derivatizing agents in environmental analysis—a critical review. *Fresenius' J. Anal. Chem.* **2000**, *366* (8), 781–791.
- (20) Behforouz, M.; Bolan, J. L.; Flynt, M. S. 2,4-Dinitrophenylhydrazones—a modified method for the preparation of these derivatives and an explanation of previous conflicting results. *J. Org. Chem.* **1985**, *50*, 1186–1189.
- (21) Lea, A. G. H.; Ford, G. D.; Fowler, S. Analytical techniques for the estimation of sulfite binding components in ciders and wines. *Int. J. Food Sci. Technol.* **2000**, *35* (1), 105–112.
- (22) Asmus, K. D.; Möckel, H.; Henglein, A. Pulse radiolytic study of the site of OH• radical attack on aliphatic alcohols in aqueous solutions. *J. Phys. Chem.* **1973**, *77*, 1218–1221.
- (23) Rashbasteq, J.; Step, E.; Turro, N. J.; Cederbaum, A. I. Oxidation of glycerol to formaldehyde by microsomes—are glycerol radicals produced in the reaction pathway. *Biochemistry* **1994**, *33*, 9504–9510.
- (24) McMorn, P.; Roberts, G.; Hutchings, G. J. Oxidation of glycerol with hydrogen peroxide using silicalite and aluminophosphate catalysts. *Catal. Lett.* **1999**, *63* (3–4), 193–197.
- (25) Carretin, S.; McMorn, P.; Johnston, P.; Griffin, K.; Kiely, C. J.; Hutchings, G. J. Oxidation of glycerol using supported Pt, Pd and Au catalysts. *Phys. Chem. Chem. Phys.* **2003**, *5*, 1329–1336.
- (26) Porta, F.; Prati, L. Selective oxidation of glycerol to sodium glycerate with gold-on-carbon catalyst: an insight into reaction selectivity. *J. Catal.* **2004**, *224*, 397–403.
- (27) Oszmianski, J.; Cheynier, V.; Moutounet, M. Iron-catalyzed oxidation of (+)-catechin in model systems. *J. Agric. Food Chem.* **1996**, *44*, 1712–1715.
- (28) Rivas-Gonzalo, J. C.; Bravo-Haro, S.; Santos-Buelga, C. Detection of compounds formed through the reaction of malvidin 3-monoglucoside and catechin in the presence of acetaldehyde. *J. Agric. Food Chem.* **1995**, *43*, 1444–1449.
- (29) Baranowski, E. S.; Nagel, C. W. Kinetics of malvidin-3-glucoside condensation in wine model systems. *J. Food Sci.* **1983**, *48* (2), 419–421.
- (30) Brouillard, R.; El Hage Chanine J. M. Chemistry of anthocyanin pigments. 6.¹ kinetic and thermodynamic study of hydrogen sulfite addition to cyanin. Formation of a highly stable Meisenheimer-type adduct derived from a 2-phenylbenzopyrylium salt. *J. Am. Chem. Soc.* **1980**, *102*, 5375–5378.

Received for review December 5, 2005. Revised manuscript received April 18, 2006. Accepted April 18, 2006. We thank the American Vineyard Foundation and the California Competitive Grant Program for providing partial funding for this project. V.F.L. is also grateful for the support of Fulbright, Laspau, Wine Spectator, Rhone Rangers, and Jastro Shields.

JF053036P